

Arylamine-Based Dyes for p-Type  
Dye-Sensitized Solar CellsYung-Sheng Yen,<sup>†</sup> Wei-Ting Chen,<sup>†,‡</sup> Chih-Yu Hsu,<sup>†</sup> Hsien-Hsin Chou,<sup>†</sup> Jiann T. Lin,<sup>\*,†</sup>  
and Ming-Chang P. Yeh<sup>\*,‡</sup>*Institute of Chemistry, Academia Sinica, Nankang, Taipei 11529, Taiwan, and  
Department of Chemistry, National Taiwan Normal University, Taipei, Taiwan 117**jtlin@chem.sinica.edu.tw; cheyeh@scc.ntnu.edu.tw*

Received July 26, 2011

## ABSTRACT



New arylamine-based sensitizers for p-type dye-sensitized solar cells (DSSCs) have been synthesized and used for p-type DSSCs. The best conversion efficiency reaches ~0.1%. Sensitizers with two anchoring carboxylic acids lead to higher open-circuit voltages, short-circuit currents, and energy conversion efficiencies.

Dye-sensitized solar cells (DSSCs) have attracted considerable attention after Grätzel's report<sup>1</sup> because of the following reasons: (1) efficient use of solar energy can meet our increasing energy demand; (2) solar energy is environmentally friendly; (3) organic sensitizers own advantages of easy production and design versatility. Up to now, DSSCs based on ruthenium dyes,<sup>2</sup> Zn-porphyrin dye,<sup>3</sup> and metal-free dyes<sup>4</sup> have promising conversion efficiencies, reaching 11 and 10%.

Sensitizers play an important role in DSSCs.<sup>5</sup> One way to improve light-harvesting of DSSCs is to use dyes absorbing in different spectral regions.<sup>6</sup> Similar to tandem organic photovoltaic cells,<sup>7</sup> tandem DSSCs with a p-type semiconductor such as NiO<sup>8</sup> as the photocathode also allow the use of dyes having complementary spectral coverage. A tandem DSSC with both electrodes photoactive is predicted to have efficiency as high as 43%.<sup>9</sup> Accordingly, there is increasing interest in p-type DSSCs.<sup>8c</sup>

<sup>†</sup> Academia Sinica.<sup>‡</sup> National Taiwan Normal University.(1) O'Reagan, B.; Grätzel, M. *Nature* **1991**, *353*, 737.(2) (a) Gao, F.; Wang, Y.; Shi, D.; Zhang, J.; Wang, M.; Jing, X.; Humphry-Baker, R.; Wang, P.; Zakeeruddin, S. M.; Grätzel, M. *J. Am. Chem. Soc.* **2008**, *130*, 10720. (b) Chen, C.-Y.; Wang, M.; Li, J.-Y.; Pootrakulchote, N.; Alababaei, L.; Ngoc-le, C.-h.; Decoppet, J.-D.; Tsai, J.-H.; Grätzel, C.; Wu, C.-G.; Zakeeruddin, S. M.; Grätzel, M. *ACS Nano* **2009**, *3*, 3103.(3) Bessho, T.; Zakeeruddin, S. M.; Yeh, C.-Y.; Diau, E. W.-G.; Grätzel, M. *Angew. Chem., Int. Ed.* **2010**, *49*, 6646.(4) Zheng, W.; Cao, Y.; Bai, Y.; Wang, Y.; Shi, Y.; Zhang, M.; Wang, F.; Pan, C.; Wang, P. *Chem. Mater.* **2010**, *22*, 1915.(5) Hagfeldt, A.; Boschloo, G.; Sun, L.; Kloo, L.; Pettersson, H. *Chem. Rev.* **2010**, *110*, 6595.(6) (a) Lee, K.-M.; Hsu, Y.-C.; Ikegami, M.; Miyasaka, T.; Justin Thomas, K. R.; Lin, J. T.; Ho, K.-C. *J. Power Sources* **2011**, *196*, 2416. (b) Fan, S.-Q.; Kim, C.; Fang, B.; Liao, K.-X.; Yang, G.-J.; Li, C.-J.; Kim, J.-J.; Ko, J. *J. Phys. Chem. C* **2011**, *115*, 7747. (c) Yum, J.-H.; Baranoff, E.; Wenger, S.; Nazeeruddin, M. K.; Grätzel, M. *Energy Environ. Sci.* **2011**, *4*, 842.(7) Ameri, T.; Dennler, G.; Lungenschmied, C.; Brabec, C. J. *Energy Environ. Sci.* **2009**, *2*, 347.(8) (a) Gibson, E. A.; Smeigh, A. L.; Le Pleux, L.; Fortage, J.; Boschloo, G.; Blart, E.; Pellegrin, Y.; Odobel, F.; Hagfeldt, A.; Hammarström, L. *Angew. Chem., Int. Ed.* **2009**, *48*, 4402. (b) Nattestad, Mozer, A. J.; Fisher, M. K. R.; Cheng, Y.-B.; Mishra, A.; Bäuerle, P.; Bach, U. *Nat. Mater.* **2010**, *9*, 31. (c) Odobel, F.; Pleux, L. L.; Pellegrin, Y.; Blart, E. *Acc. Chem. Res.* **2010**, *43*, 1063.(9) Green, M. A. *Third Generation Photovoltaics: Advanced Solar Energy Conversion*; Springer-Verlag: Berlin, Heidelberg, 2003.

The efficiencies of p-type DSSCs still remain low due to slow hole mobility in popularly used NiO electrodes and fast charge recombination and the non-ideal nature of the redox mediator, iodide.<sup>5,8c</sup> For future applications, more studies on p-type DSSCs are needed.

In p-type DSSCs, the electron pumped to the LUMO (lowest unoccupied molecular orbital) of the dye will reduce the oxidized redox mediator, and the hole of the HOMO (highest occupied molecular orbital) will inject into the valence band of NiO. Significant progress has been made on p-type DSSCs recently.<sup>8b,10</sup> Earlier, we developed some amine-based metal-free sensitizers for n-type DSSCs.<sup>11</sup> In view of the strong donating character of the arylamine moiety, we extended our studies to arylamine-based p-type sensitizers. We are interested in p-type dyes with two anchoring groups because they may not only bind the NiO surface more firmly but also facilitate hole injection. Compared to n-type congeners,<sup>12</sup> p-type sensitizers with multi-anchoring groups are still very rare.<sup>8b,13</sup> Herein we report the syntheses of new sensitizers and their applications in p-type DSSCs.

New dyes (Figure 1) synthesized are of two types: (1) with one anchoring group and one acceptor (**1**, **2**, and **3**); (2) with two anchoring groups and one acceptor (**4**, **5**, and **6**). The synthetic routes to the dyes are depicted in Scheme 1. For **1–3**, Pd-catalyzed aromatic C–N coupling<sup>14</sup> between ester-containing arylamine and formyl-containing aryl bromide proceeded first, and subsequent acidification provided carboxylic acid. Condensation of aromatic aldehyde with 1,3-diethyl-2-thioxodihydropyrimidine-4,6-dione (DETB) or malononitrile gave the final product. For **4** and **6**, Pd-catalyzed Suzuki C–C coupling<sup>15</sup> was carried out on the arylamine-containing ester. Subsequent formylation and condensation with malononitrile led to the desired product. For compound **5**, arylamine with two ester groups was synthesized from primary amine and bromobenzoate via Pd-catalyzed aromatic C–N coupling.

After formylation, the aldehyde was converted to the desired product via condensation with DETB. Pinnick oxidation<sup>16</sup> was used for oxidation of aldehyde to form carboxylic acid, and thiophene and formyl entities were incorporated in two steps to avoid using a microwave reactor. The compounds were isolated in 30–78% yields.

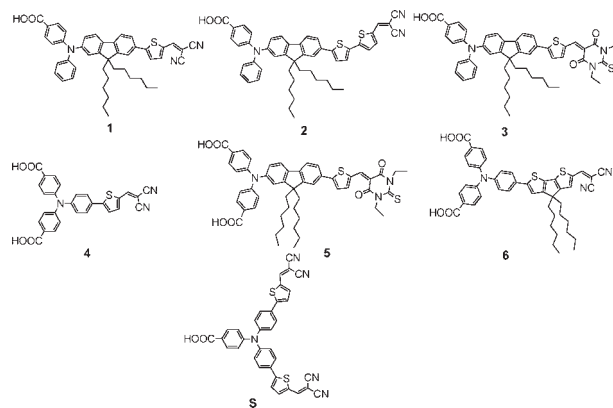


**Figure 1.** Structures of the dyes.

The absorption spectra and data are displayed in Figure 2 and Table 1, respectively. The absorption at  $> 400$  nm is attributed to  $\pi-\pi^*$  transition mixed with charge transfer transition from amine to dicyanovinyl unit. **1** and **4** have the most blue-shifted absorption among all, possibly due to the shorter spacer in the latter and the weaker acceptor in the former. Prominent red shift of the absorption spectra upon replacing the dicyanovinyl entity with 4-methylidene-3-phenylisoxazolone is consistent with the trend observed in nonlinear optical chromophores.<sup>17</sup> Slight blue shift of the absorption in **5** than in **3** can be attributed to the weakened donating power of the arylamine (vide infra) due to the presence of an extra carboxylic acid in the former. Compared with **1**, it is evident that elongation of the conjugation chain by adding extra thiophene (**2** and **6**) or extra acceptor (**S**) results in better charge delocalization. The charge transfer character in these compounds is confirmed by the density functional calculations (Table S1 and Figure S1 in the Supporting Information).

The lowest-lying electronic transitions,  $S_1$  (mainly HOMO  $\rightarrow$  LUMO), have significant oscillator strength ( $f$ ) and extent of charge separation (i.e., changes in Mulliken charge in the transition) from the arylamine to the acceptor. There is very prominent population of the HOMO at the arylamine side extending to the carboxylic acid entity, and population of the LUMOs at the dicyanovinyl side is also evident. It is interesting to note that introduction of a cyclopentadithiophene moiety (CDT) in the spacer (**6**) or an extra acceptor (**S**) increases the absorption intensity dramatically.

(10) (a) Qin, P.; Zhu, H.; Edvinsson, T.; Boschloo, G.; Hagfeldt, A.; Sun, L. *J. Am. Chem. Soc.* **2008**, *130*, 8570. (b) Qin, P.; Linder, M.; Brinck, T.; Boschloo, G.; Hagfeldt, A.; Sun, L. *Adv. Mater.* **2009**, *21*, 2993. (c) Li, L.; Gibson, E. A.; Qin, P.; Boschloo, G.; Gorlov, M.; Hagfeldt, A.; Sun, L. *Adv. Mater.* **2010**, *22*, 1759.

(11) (a) Justin Thomas, K. R.; Hsu, Y.-C.; Lin, J. T.; Lee, K.-M.; Ho, K.-C.; Lai, C.-H.; Cheng, Y.-M.; Chou, P.-T. *Chem. Mater.* **2008**, *20*, 1830. (b) Lin, J. T.; Chen, P.-C.; Yen, Y.-S.; Hsu, Y.-C.; Chou, H.-H.; Yeh, M.-C. *P. Org. Lett.* **2008**, *11*, 97. (c) Chen, C.-H.; Hsu, Y.-C.; Chou, H.-H.; Justin Thomas, K. R.; Lin, J. T.; Hsu, C.-P. *Chem.—Eur. J.* **2010**, *16*, 3184.

(12) (a) Abbotto, A.; Manfredi, N.; Marini, C.; De Angelis, F.; Mosconi, E.; Yum, J.-H.; Xianxi, Z.; Nazeeruddin, M. K.; Grätzel, M. *Energy Environ. Sci.* **2009**, *2*, 1094. (b) Heredia, D.; Natera, J.; Gervaldó, M.; Otero, L.; Fungo, F.; Lin, C.-Y.; Wong, K.-T. *Org. Lett.* **2010**, *11*, 12. (c) Sahu, D.; Padhy, H.; Patra, D.; Yin, J.-F.; Hsu, Y.-C.; Lin, J. T.; Lu, K.-L.; Wei, K.-H.; Lin, H.-C. *Tetrahedron* **2011**, *67*, 303.

(13) A paper on sensitizers with two anchoring groups appeared while this paper was in preparation: Ji, Z.; Natu, G.; Huang, Z.; Wu, Y. *Energy Environ. Sci.* **2011**, *4*, 2818.

(14) (a) Yamamoto, T.; Nishiyama, M.; Koie, Y. *Tetrahedron Lett.* **1998**, *39*, 2367. (b) Hartwig, J. F.; Kawatsura, M.; Hauck, S. I.; Shaughnessy, L. M.; Alcazar-Roman, J. *J. Org. Chem.* **1999**, *64*, 5575.

(15) (a) Miyaura, N.; Suzuki, A. *Chem. Commun.* **1979**, 866. (b) Suzuki, A. *J. Organomet. Chem.* **1999**, *576*, 147.

(16) (a) Bal, B. S.; Childers, W. E., Jr.; Pinnick, H. W. *Tetrahedron* **1981**, *37*, 2091. (b) Nakamura, S.; Sato, H.; Hirata, Y.; Watanabe, N.; Hashimoto, S. *Tetrahedron* **2005**, *61*, 11078.

(17) Jen, A. K.-Y.; Cai, Y.; Bedworth, P. V.; Marder, S. R. *Adv. Mater.* **1997**, *9*, 132.

### Scheme 1. Synthesis of the Dyes

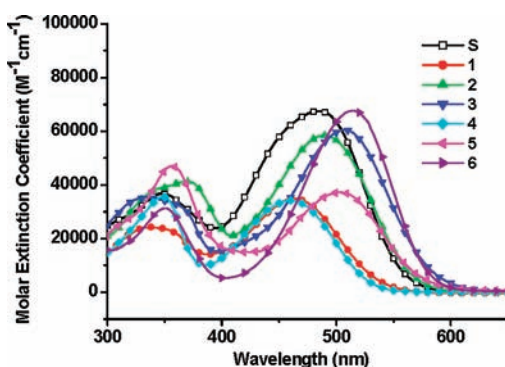
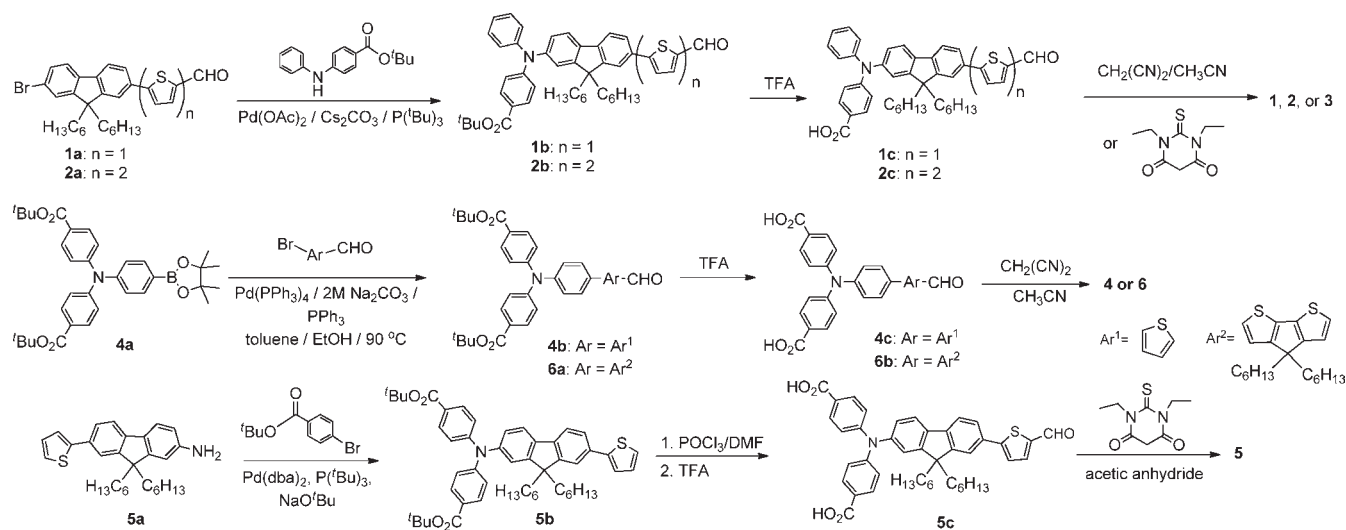


Figure 2. Absorption spectra of the dyes in tetrahydrofuran.

The electrochemical data and the cyclic voltammograms of the dyes are displayed in Table 1 and Figure S2, respectively. Except for **2** and **6**, all compounds exhibit a quasi-reversible one-electron redox wave attributable to the oxidation of the arylamine. **2** (or **6**) exhibits two quasi-reversible one-electron redox waves due to the oxidation of arylamine and bithiophene (or CDT), respectively. The first oxidation potentials ( $E_{ox}$ ) of the compounds decrease in the order of **4** > **3** > **1** > **5** > **2** > **6**. The presence of electron excessive bithiophene (or CDT) significantly lowers the oxidation potential of **2** (or **6**). In comparison, the presence of two carboxylic acids leads to a higher oxidation potential (**3**, 610 mV; **5**, 670 mV vs ferrocene) due to depletion of the electron density of arylamine. It is also evident that the stronger electron-withdrawing DETB more effectively raises the oxidation potential of arylamine than dicyanovinyl unit (**1** vs **3**). The HOMO (1.25 to  $-1.49$  V vs NHE) and LUMO ( $-0.68$  to  $-0.96$  V vs NHE) energy levels of the compounds were estimated from the oxidation

Table 1. Electrooptical Parameters of the Dyes

dye	$\lambda_{abs}$ ( $\epsilon \times 10^{-4} \text{ M}^{-1} \text{ cm}^{-1}$ ) <sup>a</sup> nm	$E_{ox}$ ( $\Delta E_p$ ) <sup>a,b</sup> mV	HOMO <sup>c</sup> , V	LUMO <sup>d</sup> , V
<b>1</b>	338 (2.46), 461 (3.51)	594 (120)	1.29	$-0.96$
<b>2</b>	340 (3.80), 369 (4.15), 489 (5.88)	565 (128), 809 (139)	1.27	$-0.89$
<b>3</b>	329 (3.59), 364 (3.18), 508 (6.08)	610 (146)	1.31	$-0.77$
<b>4</b>	348 (3.59), 460 (3.45)	790 (103)	1.49	$-0.86$
<b>5</b>	356 (4.70), 504 (3.72)	674 (111)	1.37	$-0.68$
<b>6</b>	350 (3.15), 514 (6.76)	553 (118) 715 (118)	1.25	$-0.91$
<b>S</b>	347 (3.67), 484 (6.75)	718 (137)	1.42	$-0.81$

<sup>a</sup> Recorded in THF solutions at 298 K. <sup>b</sup>  $E_{ox} = 1/2(E_{pa} + E_{pc})$ ,  $\Delta E_p = E_{pa} - E_{pc}$ , where  $E_{pa}$  and  $E_{pc}$  are anodic and cathodic potentials, respectively. Oxidation potential is referenced to that of ferrocene ( $E_{1/2}(ox) = 293$  mV vs Ag/AgNO<sub>3</sub>), which was used as an internal reference. Scan rate: 100 mV/s. <sup>c</sup> HOMO level vs NHE. <sup>d</sup> LUMO level vs NHE.

potential and the absorption band edge (Table 1). The former is below that of the top of the valence band of NiO (0.54 V vs NHE),<sup>8c</sup> and the latter is above that of the redox mediator (0.40 V vs NHE). Therefore, hole injection and dye regeneration should occur readily.

The p-type DSSCs with an effective area of 0.25 cm<sup>2</sup> nanostructured NiO film were fabricated from these dyes. The electrolyte was composed of 0.1 M I<sub>2</sub>/1.0 M LiI/0.5 M *tert*-butylpyridine in CH<sub>3</sub>CN. The device performance statistics under AM 1.5 illumination are listed in Table 2. The cell using a known sensitizer (**S**,<sup>10a</sup> Figure 1) was also fabricated for comparison. Figure S3 shows the photocurrent–voltage ( $J$ – $V$ ) curves of the cells. Figure 3 compares the incident photon-to-current conversion efficiencies (IPCE) of the dyes on NiO. The conversion

efficiencies of the cells reach 50–92% of the cell based on **S**, and the highest IPCE value is achieved by **4** (maximum of ca. 28% at 482 nm). The spectra of the dyes adsorbed on the NiO surface are shown in Figure S4. The dye adsorbing amount and the hole injection ability to the NiO result in different photocurrent output as well as light-harvesting ability. The hole injection ability can be realized through the EIS analysis of the DSSCs under illumination (Figure S5a). From the intermediate frequency semicircle ( $1-10^2$  Hz), the interfacial charge transfer resistance at the NiO/dye/electrolyte interface ( $R_{ct2}$ ) can be calculated.

**Table 2.** DSSCs Performance Parameters of the Dyes

dye	$V_{OC}$ , V	$J_{SC}$ , mA/cm <sup>2</sup>	FF	$\eta$ , %	dye loading, $10^{-7}$ mol/cm <sup>2</sup>	$R_{ct2}$ , $\Omega$
<b>1</b>	0.105	1.59	0.359	0.060	1.53	183
<b>2</b>	0.115	1.39	0.363	0.058	1.58	160
<b>3</b>	0.113	1.38	0.340	0.053	1.54	223
<b>4</b>	0.125	2.25	0.331	0.093	1.30	124
<b>5</b>	0.122	2.18	0.346	0.092	1.19	134
<b>6</b>	0.131	2.05	0.324	0.087	1.08	135
<b>S</b>	0.132	2.31	0.331	0.101	1.29	146

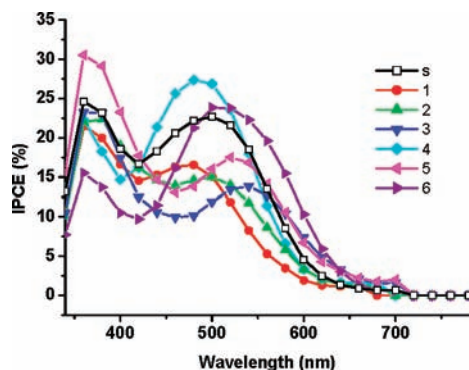


**Figure 3.** IPCE plots for the DSSCs using PT and S dyes.

The  $R_{ct2}$  values obtained by employing the equivalent circuit for the curves fitted the impedance spectra of the DSSCs (Figure S5a) are listed in Table 2 along with the dye loading amount. **1–3** have higher dye density on NiO

(18) Morandier, A.; Boschloo, G.; Hagfeldt, A.; Hammarström, L. *J. Phys. Chem. C* **2008**, *112*, 9530.

surface but lower photocurrent compared to others, possibly due to less efficient hole injection or light harvesting. Despite blue-shifted absorption spectra, **4** has high photocurrent output, which is consistent with its low  $R_{ct2}$  value. The low  $R_{ct2}$  values of **5** and **6** are also attributed to the presence of two anchoring groups.

The dyes with two anchoring groups (**4** to **6**) that have significantly higher open-circuit voltages deserve attention. The low efficiency of DSSC based on C343 was attributed to a fast charge recombination of the reduced dye with the hole in the valence band of NiO instead of charge recombination between the electrolyte and the hole (dark current).<sup>18</sup> We believe that suppression of dark current may be also taken into consideration for the cell performance. More efficient suppression of dark current of N719 than Z907 was suggested to be due to more effective coverage of TiO<sub>2</sub> for prevent electrolytes from approaching the TiO<sub>2</sub> surface.<sup>19</sup> Similarly, the two anchoring groups in **4–6** may effectively cover the naked NiO surface from being exposed to the electrolyte.

Our argument is supported by the EIS measured in the dark (Figure S5b). The intermediate frequency semicircle represents the charge transfer phenomena between the NiO surface and the electrolyte (i.e., dark current). Efficient suppression of the dark current leads to a larger semicircle. Variation of the NiO Fermi level caused by the surface dipole cannot be excluded, however.<sup>20</sup> Two carboxylic groups facilitate hole injection, as evidenced from the HOMO of the molecule, which has an electron population extending to the carboxylic groups (vide supra). Besides suppression of dark current, sensitizers with two anchoring groups may also enhance dye bonding on the surface of the photoelectrode.

In conclusion, new arylamine-based sensitizers for p-type DSSCs have been synthesized. The p-type DSSCs using these sensitizers and NiO as the photocathode have efficiencies ranging from 0.053 to 0.093%. The sensitizers with two anchoring carboxylic acids have higher  $V_{OC}$  and  $J_{SC}$  values as well as better efficiencies.

**Acknowledgment.** We acknowledge the support of the Academia Sinica (AC) and NSC (Taiwan), and the Instrumental Center of Institute of Chemistry (AC).

**Supporting Information Available.** Synthetic procedures and characterization for new compounds. This material is available free of charge via the Internet at <http://pubs.acs.org>.

(19) Mori, S. N.; Kubo, W.; Kanzaki, T.; Masaki, N.; Wada, Y.; Yanagida, S. *J. Phys. Chem. C* **2007**, *111*, 3522.

(20) (a) Heimel, G.; Romaner, L.; Zojer, E.; Bredas, J.-L. *Acc. Chem. Res.* **2008**, *41*, 721. (b) Braun, S.; Salaneck, W. R.; Fahlman, M. *Adv. Mater.* **2009**, *21*, 1450.